NASA Technical Memorandum 105321
AIAA–92–0152

A Study on Vortex Flow Control on Inlet Distortion in the Re-Engined 727-100 Center Inlet Duct Using Computational Fluid Dynamics

Bernhard H. Anderson
Lewis Research Center
Cleveland, Ohio

and

Pao S. Huang, William A. Paschal, and Enrico Cavatorta
The Dee Howard Company
San Antonio, Texas

Prepared for the
30th Aerospace Sciences Meeting and Exhibit
sponsored by the American Institute of Aeronautics and Astronautics
Reno, Nevada, January 6–9, 1992

NASA

A STUDY ON VORTEX FLOW CONTROL OF INLET DISTORTION IN THE RE-ENGINED 727-100 CENTER INLET DUCT USING COMPUTATIONAL FLUID DYNAMICS

by

Bernhard H. Anderson
NASA Lewis Research Center
Cleveland, OH 44135

Pao S. Huang, William A. Paschal, and Enrico Cavatorta
The Dee Howard Company
San Antonio, TX 78217

ABSTRACT

In this preliminary research study, computational fluid dynamics (CFD) was used to investigate the management of inlet distortion by the introduction of discrete vorticity sources at selected locations in the inlet for the purpose of controlling secondary flow. These sources of vorticity were introduced by means of vortex generators. A series of design observations were made concerning the importance of various vortex generator design parameters in minimizing engine face circumferential distortion. The study showed that vortex strength, generator scale, and secondary flow field structure have a complicated and interrelated influence on the engine face distortion, over and above the initial geometry and arrangement of the generators. Overall, the installed vortex generator performance was found to be a function of three catagories of variables, namely: (1) the inflow conditions, i.e. throat Mach number (inlet mass flow), Reynolds number, etc., (2) the aerodynamic characteristics associated with the inlet duct, and (3) the design parameters related to the geometry, arrangement, and placement of the vortex generators within the inlet duct itself.

INTRODUCTION

In the re-engining program for the 727-100 aircraft, the TAY650 series engines were chosen to replace all the current existing engines to reduce the jet noise and specific fuel consumption. In order to accomplish this goal, a major engineering effort was initiated to design a new inlet S-duct for the center engine in order to deliver the 30% increase in air mass flow required by the TAY650 series engines. The design goals for the new inlet included a minimum total pressure recovery of 0.960 and engine face distortion level consistent with stable engine operation, without modifications to the existing 727-100 aircraft structure. Both total pressure recovery and inlet distortion are influenced by the viscous behavior of fluids, and in particular, by the development of secondary flow within the inlet duct.

One of the most commonly used methods to control local boundary layer separation within diffusing ducts is the placement of vortex generators upstream of the problem area. Vortex generators in use today are small wing sections mounted on the inside surface of the inlet inclined at an angle to the oncoming flow to generate a shed vortex. The generators are usually sized to the local boundary layer height for the best interaction between the shed vortex and boundary layer, and are usually placed in groups of two or more upstream of the problem area. The principle of boundary layer control by vortex generators relies on induced mixing between the external or core stream and the boundary layer. This mixing is promoted by vorticies trailing longitudinally near the edge of the boundary layer. Fluid particles with high momentum in the stream direction are swept along helical paths toward the duct surface to mix with and, to some extent, replace the low momentum boundary layer flow. This is a continuous process that provides a source of re-energization to counter the natural boundary layer growth caused by friction, adverse pressure gradients, and low energy secondary flow accumulation.

There are two basic configurations of vortex generators. In one configuration, all the vortex generators are inclined at the same angle with respect to the oncoming flow direction. These are called co-rotating configurations because the shed vorticies rotate in the same direction. In the other configuration, the vortex generators are grouped in pairs inclined in opposite direction, such that pairs of counter-rotating shed vorticies are generated.

Co-rotating vortex generators are very useful in reducing flow separation if the generators are properily selected and located. The main advantage of co-rotating type vortex generators are their downstream effectiveness resulting in more effective usage of the vortex energy within the affected boundary layer. According to design 'wisdom', this type of vortex generator has a few special advantages when used within S-duct inlet configurations, namely: (1) the induced vortices will remain close to the wall; consequently a 'cleaner' core flow will result, and (2) the induced vorticies will counteract the natural and often strong secondary flows which can develop.

Counter-rotating, equal strength vortex generators have been used in a number of aircraft inlet ducts, including the F/A-18 and the 727. This type of vortex generator is very effective in reducing flow separation if the vortex generators are placed slightly upstream of the region of separation. However, according to vortex generator design 'wisdom', the disadvantages of this type of generators, as compared to co-rotating generators, are that the induced vorticies tend to lift off the duct surface, thus reducing their effectiveness, causing higher loss in inlet recovery and larger total pressure distortion at the compressor face.

The performance of vane-type vortex generators was evaluated by Taylor (Ref. 3), for diffusers and airfoils at low speed, and by Valentine and Carrol (Refs. 4 and 5), for airfoils and wings at high speeds. This work provides trends in effectiveness for certain vortex generator design variables such as angle-of-attack, height, and distance ahead of separation. Attention was focused on the detailed changes that were produced in the boundary layer as a result of placement of vortex generators in the flow. Percy and Stuart (Ref. 6), extended the study of the effects of various design parameters and concluded that the strength and disposition of the individual induced vortices was more important than the details of the boundary layer upstream of the imposed pressure gradient.

It was not until the confirmation test by Kaldschmidt, Syltebo, and Ting (Ref. 7), on the 727 center inlet duct for the refanned JT8D engine that an attempt was made to use vortex generators to restructure the development of secondary flow in order to improve the engine face distortion level.

With this work, a very important shift in strategy on the use of vortex generators had occurred. The perspective had shifted from a local one, in which the goal was to prevent boundary layer separation, to a global one, in which the goal was to control secondary flow in order to minimize engine face distortion.

In order to accomplish this new objective for internal flow control, the design strategy must shift from an experimental to an analysis based methodology. This paper represents one in a series of studies (Refs. 8-11), on the design issues associated with inlet-engine compatibility problems, and in particular, engine face distortion and its control. These studies center on the development of CFD tools and techniques for use within an analysis-design enviornment, an the application of these new analysis approaches to understand and control inlet-engine distortion. The first paper in this series, by Anderson (Ref. 8), dealt with the aerodynamic characteristics of vortex interaction within the F/A-18 inlet duct, where the vortex interaction arises as a result of a vortex ingestion. Later studies will involve the effect of vortex ingestion on the engine face flow field itself. The second paper in this series, by Anderson and Levy (Ref. 9), demonstrated that an installation of co-rotating vortex generators could be constructed to tailor the development of secondary flow to minimize engine face distortion. Of importance is the conclusion that there exists an optimum axial location for the co-rotating vortex generators, and a maximum spacing of the generators above which the engine face distortion rapidly increases. This study also showed that the vortex strength, generator scale, and secondary flow field structure have a complicated and interrelated influence on the engine face distortion, beyond the initial arrangement of generators. The third paper in this series, by Anderson and Farokhi (Ref. 10), concluded that there exists a class of streamwise separated flows which are dominated by the transport of vorticity, and such separations, termed 'vorticity separations', are associated with vortex liftoff. These separated flows are very common in inlet ducts, and are a major cause of pressure loss and engine face distortion. Reduced Navier Stokes (RNS) solution techniques were shown to describe the topological and topographical features of such flow separations, and the numerical results were very consistent with those from two Full Navier Stokes (FNS) codes with regard to the separation point and reattachment length. Because of the large number of independant variables associated with the design of vortex generator systems for flow control, the fourth paper in this series by Anderson and Levy (Ref. 11), examined the use of numerical optimization procedures to assist the engineer in this process. A performance parameter was suggested to account for both inlet distortion and total pressure loss at a series of design flight conditions.

The overall objective of this paper is to advance the understanding, the prediction, and the control of inlet distortion, and to study the basic interactions that influence this important design problem. Specifically, the goals of the present paper are: (1) to demonstrate the capability of the Reduced Navier Stokes code RNS3D assist in the design of the vortex generator system for the new center inlet duct for the 727-100 series aircraft, (2) to investigate the effects of inlet flow conditions and the geometry, arrangement, and placement of vortex generators on engine face distortion, and (3) to make some formal observations concerning the importance of various vortex generator installation parameters in minimizing engine face distortion.

THEORETICAL BACKGROUND

The flow through the S-duct inlet is computed by solving the Reduced Navier Stokes (RNS) equations using the RNS3D computer code. Solution proceedures similar to this have also been referred to as parabolized, partially-parabolized, or semi-elliptic procedures. The RNS equations are derived using approximations from the velocity-decomposition approach of Briley and McDonald (Refs. 12-13). For the cases being considered, these equations yield accurate flow predictions, while reducing the labor of solution below that required for the full Navier-Stokes equations. The equations are solved by an efficient spatial forward marching procedure. Unlike the partially-parabolized or semi-elliptic procedures, a single sweep through the inlet is used in the solution procedure. This solution technique has been validated over a wide range of conditions (Refs. 14-18). Further details on the RNS3D computer code may be found in Ref. 8.

Vortex Generator Model

The model for the vortex generators within the RNS analysis, described by Kunik, (Ref. 19), takes advantage of the stream function-vorticity formulation of the governing equations. The shed vortex is modeled by introducing a source term into the vorticity equation that is a function of the geometric characteristics of the generators themselves. This source term is introduced at every point in the cross-plane in the form of the following expression

$$\Gamma_p = \Gamma_0 e^{-(c_1 r^2)} \tag{1}$$

where Γ_p is the vortex strength at any point in the cross-plane, Γ_0 is the vortex strength at the tip of the generator, r is the distance between the field point and the tip of the generator, and c_1 is a constant which controls the decay of the shed vortex strength in the cross-plane. The geometry of the generator is related to the vortex strength at the blade tip through the term Γ_0, defined by

$$\Gamma_0 = 8.0 \rho u c \tanh(\alpha) \tag{2}$$

where ρ is the fluid density, u is the velocity of the flow at the generator tip, c is the chord length, and α is the aerodynamic angle of attack in radians. The decay constant c_1 in Equ. (1) is given by the expression

$$c_1 = 4.0/c^2 \tag{3}$$

This vortex model resembles the one proposed by Squire (Ref. 20), except that it neglects the variation of viscosity in the cross-plane. Kunik (Ref. 19), found that this vortex generator model showed "good qualitative agreement with idealized and experimental results" and that the "distortion levels and alleviation of separation also agreed with experimental results".

Steady State Engine Face Distortion Descriptors

It is impractical to measure anything at the engine face when the engine is installed and operating, consequently, the engine and inlet designers agreed upon an Aerodynamic Interface Plane (AIP) which is forward of the compressor face but sufficiently close to the engine face to have a similar flow field. Current U.S. practice uses forty or forty eight transducer probes arranged in eight rakes with five or six rings. The radius of each ring is set such that all probes are at the centroid of equal areas. All distorton descriptors, whether they quantify steady state or transient distortion conditions, are always calculated relative to the standard rake located at the AIP. In experimental data reduction, it is assumed that the both the static pressure and temperature are constant and steady across the AIP; thus both the velocity and Mach number can be considered functions only of total pressure and the distribution of this quantity is the only measurement that needs to be made.

The most widespread quantitative distortion descriptor available in the literature, because of its use in the earliest measurements on inlet ducts in the late 1950's, is simply:

$$Dt = \left(\frac{Pt_{max} - Pt_{min}}{Pt_{ave}} \right) \quad (4)$$

where Pt_{max} is the maximum measured total pressure, Pt_{min} is the minimum total pressure, and Pt_{ave} is the area weighted average total pressure. This descriptor indicates the maximum variation in total pressure across the AIP and is useful to describe the 'general health' of inlet ducts irrespective of the type of powerplant that may be used.

More advanced distortion descriptors, introduced in the late 1960's and 1970's, take into account the radial and circumferential total pressure variation across the AIP. The effect of circumferential distortion on compressor surge margin is essentially to drop the maximum pressure ratio of a constant corrected speed line. One of the simplest quoted descriptors for circumferential distortion is from Rolls Royce and is defined as

$$DC_\theta = \left(\frac{Pt_{ave} - Pt_{min}}{q_{ave}} \right) \quad (5)$$

where typical values of θ are 60.0°, 90.0°, and 120.0°, Pt_{min} is the minimum total pressure in any section of extent θ, Pt_{ave} the average total pressure and q_{ave} is the average dynamic pressure evaluated at the aerodynamic interface plane. For bypass engines, a circumferential distortion descriptor $DC_{\theta-GG}$ is often used, where GG indicates that the index is taken over the area of the gas generator.

The radial distortion Dt_r is defined as

$$Dt_r = \left(\frac{Pt_{max} - Pt_{ave}}{Pt_{max}} \right)_{ring} \quad (6)$$

where Pt_{ave} is the average total pressure for a given ring radius and Pt_{max} is the maximum local ring total pressure. The distortion parameter Dt_θ contains information of both radial and circumferential distortion and is defined as:

$$Dt_\theta = \left(\frac{Pt_{ave} - Pt_{min}}{Pt_{ave}} \right)_{ring} \quad (7)$$

where Pt_{min} is the lowest average total pressure in any θ segment, usually 60° or 180° of arc for a given ring radius having an average ring total pressure Pt_{ave}.

RESULTS AND DISCUSSIONS

The Design Problem in the Control of Inlet Distortion

Unlike external aerodynamics where the two-dimensional flow assumption is valid over extended regions of the flow field, the internal flow problem is plagued with three-dimensional flow effects. When viscous effects or other sources of vorticity are present, three-dimensional flows differ fundamentally from their two-dimensional counterparts in that large secondary flows are generated by a deflection of the primary flow and/or other mechanisms. Secondary flow theory (reviewed by Horlock and Lakshminaryana Ref. 22, and Lakshminarayana and Horlock Ref. 23) affords considerable insight into the generation of secondary flow and establishes that large secondary flows can be generated by small deflection of vorticity or shear. The large secondary flows thus generated often exert an appreciable influence on the primary flow, and thus aerodynamic performance, viscous losses, and engine face distortion can be significantly affected. Thus the design problem is controlling the three dimensional secondary flows that are generated within inlet ducts by introducing discrete sources of vorticity through an arrangement of vortex generators. This defines the concept of vortex flow control. The purpose of this installation is to minimize engine face distortion, and the effectiveness of the design is determined by standard distortion descriptors such as the DC_{60} indicator.

Installed Vortex Generator Performance Characteristics

The application of the three-dimensional Reduced Navier Stokes code RNS3D to analyze and design a new center inlet S-duct for the 727-100 series aircraft using the TAY651-54 engines is described by Huang and Piccolo (Ref. 24), and by Huang, Picollo, Paschal, and Anderson (Ref. 25). The starting point for new center inlet was the original S-duct geometry described by Kaldschmidt, Syltedo, and Ting (Ref. 7), for the JT8D series engines. In order to arrive at the new S-duct geometry, a sensitivity study was conducted and six categories of geometry perturbations were studied which included:

(1) Variation of the area distribution in the first bend.

(2) Variation of the area distribution in the second bend.

(3) Variation of the area distribution in both bends.

(4) Variation in the centerline radius of the first bend.

(5) Modification of the cross-sectional shape to super-elliptic throughout the duct.

(6) Modification of the cross-sectional shape to elliptic from the inlet to the spar station.

The results of this study showed that perturbations of the area distribution and centerline shape in the upstream section of the duct had major effects on the aerodynamic characteristics of the inlet. Thus, by raising the inlet duct centerline to increase the radius in the first bend and altering the area distribution to accomodate the increase airflow requirements and dimensions of the TAY651 engines, a separation free inlet duct was designed which had high recovery and low distortion. It is this inlet S-duct configuration that is used in the present study on vortex flow control of inlet distortion.

The inlet duct geometry and computational grid used in the present study is shown in Fig. 1. A polar grid was chosen for this S-duct which consisted of 49 radial, 49 circumferential, and 241 streamwise nodal points in the half plane, for a total number of mesh points of 578,641. The CPU time was 13.5 minutes on the CRAY XMP for this number on mesh points. The internal grid was constructed such that the transverse computational plane was perpendicular to the duct centerline. Grid clustering was used in the radial direction to redistribute the nodal points to resolve the high shear regions near the wall. The flow in the inlet was turbulent throughout, with an initial shear layer thickness δ/D_i of 0.005.

The geometry of the co-rotating vortex generators used in this study along with the nomenclature used in positioning the individual blades are presented in Figs. 2 and 3. The important geometric design parameters include: (1) the vortex generator blade height h/R_i, (2) the blade chord length c/R_i, and (3) the vane angle-of-attack β_{vg}. Instead of the usual spacing parameter d/R_i, i.e. the distance between adjacent blades, the positioning of the vortex generator blades was described in terms of a spacing angle α_{vg} and a sector angle over which the blades were positioned θ_s. For this study, the relationship between blade spacing angle α_{vg} and sector angle θ_s is given by

$$\theta_s = \alpha_{vg}\left(n_{vg} - \frac{1}{2} \right) \quad (9)$$

where n_{vg} is the number of vortex generator blades. Equ. (9) wás also used to position the individual generator blades around the inside periphery inlet within the half plane grid. The angle θ, was measured counter-clockwise relative to an azimuthal angle of 180° with respect to the vertical axis of the duct. It should be remembered that only a half-plane calculation was performed in this study, and Equ. (9) is used to place the individual vortex generators within that half-plane computational grid. Thus, the total number of vortex generators within the real inlet is twice the number actually used in the calculation. Since the other half of the inlet is the mirror image of the computational inlet, each co-rotating generator can be view as having a corresponding mirror image, i.e. the co-rotating vortex generators can be labeled as pairs. Shown in Fig. 4 are the axial locations of the vortex generator sector regions covered in this study. These sector regions were positioned between $X_{vg}/R_i = 2.0$ and $X_{vg}/R_i = 6.0$ and covered a sector angle θ, up to 157.5° in the half-plane computational grid, or 315.0° in the real duct.

Figs. 5 and 6 show a comparision between the measured and calculated engine face total pressure recovery and engine face DC_{60} distortion for the inlet without vortex flow control. The calculated performance is shown as a function of inlet throat Mach number M_i at an inlet Reynolds number of Rey of $12.15x10^6$ based on inlet diameter D_i. For the entire range of Mach numbers considered, the analysis indicated the flow remained attached. Under these conditions, RNS3D was able to predict the total pressure recovery and DC_{60} engine face distortion index very well at the designated critical flight condition.

The 727/TAY651-54 center inlet S-duct design, described in Refs. 24 and 25, was composed of the two sets of vortex generator configurations, a forward co-rotating configuration defined by

Number of Generator Pairs:	$n_{vg} = 9$
Generator Sector Location:	$X_{vg}/R_i = 3.0$
Generator Blade Height:	$h/R_i = 0.050$
Generator Chord Length:	$c/R_i = 0.181$
Generator Spacing Angle:	$\alpha_{vg} = 15.0°$
Vane Angle-of-Attack:	$\beta_{vg} = 15.0°$
Generator Sector Angle:	$\theta_s = 127.5°$

and a rearward counter-rotating configuration defined by:

Number of Generator Pairs:	$n_{vg} = 7$
Generator Sector Location:	$X_{vg}/R_i = 5.0$
Generator Blade Height:	$h/R_i = 0.050$
Generator Chord Length:	$c/R_i = 0.119$
Generator Spacing Angle:	$\alpha_{vg} = 15.0°$
Vane Angle-of-Attack:	$\beta_{vg} = 15.0°$
Generator Sector Angle:	$\theta_s = 97.5°$

The aerodynamic performance of the inlet with both sets of generators was predicted by RNS3D and reported by Huang and Piccolo (Ref. 24), and by Huang, Picollo, Paschal, and Anderson (Ref. 25). This is the first example where computational fluid dynamics (CFD) was used to design a vortex generator installation prior to wind tunnel testing and final flight certification.

Shown in Figs. 7 and 8 are a comparision between the measured and calculated total pressure recovery and engine face DC_{60} distortion with vortex flow control. The recovery characteristics shown in Fig. 7 are for the forward and rearward generator configurations installed in the inlet based on both an area weighted and mass flow weighted average total pressure at the engine face station. The DC_{60} distortion characteristics shown in Fig. 8 are for two generator configurations, namely (1) the forward configuration alone, and (2) the forward and rearward generator configurations installed in the inlet. The calculated performance is shown as a function of inlet throat Mach number M_i at an inlet Reynolds number Rey of $12.71x10^6$.

Similar to the rational used in Ref. 7, the rearward generator installation was used to surpress a natural occuring boundary build-up along the top of the inlet duct as a result of secondary flow. Overall, the rearward installation of vortex generators reduced DC_{60} engine face distortion by an average value the of less than 0.002 (shaded area in Fig. 8) from that obtained from the forward generator configuration alone, over the inlet throat Mach number range from 0.1 to 0.6. In general, it is very difficult to substantially influence the engine face distortion characteristics with a generator installation positioned that far downstream in the inlet duct.

Three important conclusions can be reached from Figs. 7 and 8, namely: (1) 3D RNS solution methods can predict overall inlet performance very well at the designated critical operating point, (2) the forward co-rotating vortex generator installation alone had major influence the over distortion level at the engine face, and (3) vortex generators are a very low loss method for controlling engine face distortion. The measured total pressure loss as a result of the two vortex generator installation composed of a total of thirty two (32) vane-type vortex generators was less than 0.002. This is consistent with the measured losses reported in Ref. 7, which was 0.002 for twenty six (26) vane-type vortex generators.

Aerodynamic Properties of Inlet Distortion

The effect of inlet throat Mach number on the DC_{60} engine face distortion for the baseline S-duct configuration is shown with the engine face recovery map at each computed throat Mach number in Figs. 9 and 10. These calculations were performed at a Reynolds number of $12.71x10^6$. Without vortex flow control the strength of the secondary flow decreases with decreasing throat Mach number, with the net result that there is a decrease in DC_{60} engine face distortion. This results from the fact that the strength of the induced secondary flow is decreasing faster with inlet throat Mach number than the average dynamic pressure at the engine face (see discussion below). However, the interaction between the induced secondary flow and vortex flow established by the generator installation is such that the combined secondary flow decreases more slowly with the average engine face dynamic pressure than the secondary flow field without vortex generators. Thus, the combined flow field causes a slightly increasing DC_{60} engine face distortion with decreasing inlet throat Mach number, and a secondary flow field that behaves very differently from that obtained without vortex generators. It is apparent that the overall effect of the vortex generator installation is to suppress the Mach number influence on the engine face distortion as measured by the DC_{60} descriptor. Thus, the introduction of vortex flow control has changed the aerodynamic properties of secondary flow development, and consequently, engine face distortion characteristics.

It is important to indicate that the DC_{60} distortion descriptor, defined by Equ. (5), has the interesting property that both the numerator (defined by the pressure difference $Pt_{ave} - Pt_{min}$) and the denominator (define by the average dynamic pressure q_{ave} at the engine face) both approach zero as the inlet throat Mach number approaches zero. In addition, in examining inlet throat Mach number effects on DC_{60} engine face distortion, it is important to understand that what is being measured is a pressure difference relative to an average engine face dynamic pressure, both of which decrease differently with Mach number. The pressure difference $Pt_{ave} - Pt_{min}$ is affected by inlet throat Mach number in two ways, namely (1) as a compressibity effect, and (2) as changes in the strength and the development secondary flow. It is the changes in the strength and development of secondary flow over the flight envelopee that is the very heart of understanding inlet distortion.

Observations on Vortex Generator Installation Design

The relative engine face distortion levels at different flight conditions is important since inlets must be designed to to operate with low distortion over a flight envelope. Trades between what is needed at one flight condition, such as takeoff, and what is needed at other conditions, such as transonic maneuvering at low altitudes, or cruise, must be made. Reynolds number, Mach number, inlet mass flow and engine tolerance can all change from one operating condition to another. Except where indicated, these studies were conducted at an inlet throat Mach number of 0.60 and Reynolds number of $16.0x10^6$ based on inlet diameter. The standard blade section used in this study was composed of a low aspect ratio flat-plate vane type generator, where the ratio of blade height to chord length h/c was fixed at 0.259, and the vane angle-of-attack β_{vg} was set at 16.0°. Although not part of this study, it has been found that the strength of the individual vortex from the generator blade does not vary rapidly with vane angle-of-attack β_{vg} for low aspect ratio vanes, and so the system is relatively insensitive to changes in local flow direction on the surface. This is in agreement with the conclusions reached by Pearcy (Ref. 6), who obtained his information from experimental measurements.

For the purposes of this study, the performance characteristics of only the forward installation of co-rotating vortex generators (designated in this paper as configuration dh729) will be studied, since this installation has major influence over inlet flow field structure. This is in keeping with the results of the inlet duct sensitivity study previously discussed, as well as the conclusions reached about the influence of the rearward generator configuration. A study of the rearward counter-rotating installation and its aerodynamic characteristics is a major effort and will be left for another article.

The effect of vortex generator axial sector location X_{vg}/R_i on DC_{60} engine face distortion is presented in Fig. 11 for an installation composed of nine co-rotating generator pairs spaced over a a sector angle of 127.5° according to Equ. (9). The generator spacing angle α_{vg} was thus 15.0°. For this installation of vortex generators, the position which minimizes DC_{60} engine face distortion lies between an axial position of 5.0 and 6.0, with an overall distortion level of 0.01. The total pressure recovery maps shown in Fig. 11 indicate the manner in which the performance changes with axial position and suggests that this generator installation over compensated for the effects of secondary flow at an axial location of 2.0, and under compensated for the effects of secondary flow at an axial location of 6.0. This characteristic leads to the first and most important of a number of design observations which can be stated as follows:

For a given geometry and arrangement of vortex generators, there exists an axial location which will minimize engine face distortion at a given inlet flow condition.

Presented in Fig. 12 is the effect of Reynolds number on the optimum axial installation location for the same basic vortex generator configuration as described for Fig. 11. The computations were performed at Reynolds numbers of $8.0x10^6$, $12.0x10^6$, and $16.0x10^6$, and indicate that the optimum axial sector location tends to move upstream with decreasing Reynolds number. The Reynolds number effect on installed performance characteristics suggests that an acceptable position for this generator configuration would lie between the axial stations of 3.0 and 4.0. This generator installation location will result in low engine face circumferential distortion over a wide range of Reynolds numbers. The second of the design observations in this set can thus be stated as follows:

For a given geometry and arrangement of vortex generators, there exists an axial location which will minimize the Reynolds number effect on engine face distortion.

Shown in Fig. 13 is the effect of blade height on the optimum axial sector location for the same basic vortex generator configuration as described for Figs. 11 and 12. Computations were performed at blade heights of 0.040, 0.045, and 0.050 and axial sector stations between 2.0 and 6.0. In general, as the vortex generator blade height is decreased, the optimum axial sector location moves upstream and the distortion becomes more sensitive to perturbation in that axial position. The engine face recovery maps shown in Fig. 13 at the optimum axial sector locations of 3.5, 4.0 and 5.0 are remarkably similar and the DC_{60} distortion varies less than 0.005 between those three points. The third observation thus becomes:

There exists more than one vortex generator configuration and axial position that will minimize engine face distortion to within 0.005 of each other.

Fig. 14 presents the effect of vortex generator blade height on the DC_{60} engine face distortion for the generator installation located at $X_{vg}/R_i = 3.0$. The calculations were performed at an inlet throat Mach number of 0.60 and Reynolds number of 16.0°. In general, the installed characteristics indicate that the performance of 'under compensating' generator installations degrades much faster than 'over compensating' installations. In fact, the engine face distortion as measured by the DC_{60} indicator is quit acceptable over a range of generator heights from 0.040 to 0.055, at this inlet flow condition. Thus, the installed performance characteristics shown in Fig. 14 illustrate the fourth observation which can be stated as follows:

For a given configuration of vortex generators positioned at a fixed axial location, there exists a blade height which will minimize the engine face distortion.

Fig. 15 presents the effect of vortex generator spacing angle α_{vg} on the DC_{60} engine face distortion for a generator installation located at $X/R_i = 3.0$. Also shown are the individual engine face recovery maps at the spacing angles considered in the analysis. The calculations were performed at an inlet throat Mach number of 0.60 and Reynolds number of $16.0x10^6$ For this sequence, the generator sector angle θ, was held fixed at 157.5°, while the spacing is determined by Equ. (9) for a given number of vortex generator pairs. The spacing of the individual generator blades around the inside periphery of the inlet duct was also determined by Equ. (9). For this set of inlet flow conditions, vortex generator geometry, installation location, and inlet duct aerodynamic characteristics, there exists a generator spacing angle which will minimize the DC_{60} engine face circumferential distortion. It is important to realize that this optimum spacing angle can occur any point within a 'reasonable' set of spacing angles that would be chosen for a given design. This is illustrated in Fig. 16, which shows a comparison between the spacing angle characteristics for the 727/TAY651-54 center inlet duct and the RAE2129 intake, (Ref. 26). This optimum spacing angle is clearly a function of inlet Reynolds number as revealed in Fig. 17. In general, for a given generator blade geometry and installation location, the optimum spacing angle will decrease with decreasing Reynolds number, as shown in Fig. 17. Summarizing, the fifth design observation can be expressed as follows:

For a given configuration of vortex generator positioned at a fixed axial location, there exists a spacing angle which will minimize engine face distortion, and this optimum angle can can occur at any point within a 'reasonable' set of spacing angles chosen for the design.

Presented in Fig. 18 is the effect of vortex generator sector angle on the DC_{60} engine face distortion index at an axial sector location of 3.0, and spacing angle of 15.0°. As the number of vortex generators increases, at a constant spacing angle, the sector angle will increase according to Equ. (9). This has the effect of 'spreading' the low energy flow more evenly around the the engine face, and decreasing the engine face circumferential distortion. Therefore, the more co-rotating generators that are installed around the periphery of the inlet duct, the more uniform the distortion pattern that can be realized at the engine face. This can clearly be seen from the engine face distortion maps presented in Fig. 18. However, depending on the engine face distortion descriptor, and the sector angle over which the averaging process takes place, a 'local optimum' can occur as is indicated in Fig. 18. It is this characteristic that makes numerical optimization techniques difficult to apply to vortex generator installation design. Although not shown, a 'local optimum' can also occur in the engine face distortion as a function of generator spacing angle α_{sg}. In summary, the sixth design observation can be stated as follows:

The sector angle at which the minimum engine face distortion occurs will be at least 360° although a 'local optimum' can occur depending on the chosen distortion descriptor and angle over which the averaging process takes place.

The Aerodynamics of Vortex Flow Control

The Reduced Navier Stokes (RNS) solution showing the engine face flow field and limiting streamline pattern for the inlet duct without vortex generators is presented in Figs. 19 and 20. Calculations were performed for an inlet throat Mach number of 0.519, and Reynolds number of $12.15x10^6$. The coalescence of the streamlines in Fig. 20 is indicative of a secondary flow separation, and is caused by the development of a very strong vortex pair in the first half of the duct. It is this phenomena that accounts for the sensitivity of the inlet duct design to perturbations in the geometry of the forward section, and suggests why vortex flow control is very effective when used in the forward section of the inlet. This vortex pair 'sweeps' the low energy boundary layer flow from the inside surface into the vortex core, causing circumferental distortion at the engine face. This vortex pair can be clearly seen in Fig. 19. In some instances, this vortex pair can 'lift-off' from the inside surface of the inlet duct, thereby greatly aggravating the engine face distortion problem. The flow physics of 'vortex lift-off', which is a common phenomena in 3D inlet ducts, is discussed by Anderson (Ref. 10), including the analysis of this interaction using the Reduced Navier Stokes equations.

Figs. 21 and 22 present the engine face flow field and limiting streamline pattern that result with the dh729 vortex generator configuration installed in the inlet. The analysis of this vortex generator installation was performed at an inlet throat Mach number of 0.520 and Reynolds number of $12.71x10^6$ based on inlet diameter. The effect of this generator installation was to 'spread out' the low energy flow more evenly around the inside periphery if the engine face, Fig. 21. This had consequences for the limiting streamline pattern, as can be seen by comparing Figs. 18 and 22.

Presented in Figs. 23 and 24 are the engine face flow field and limiting streamline pattern obtained with the dh733 vortex generator installation. This vortex generator installation is the same as config. dh729, except that it is positioned at an axial station of 5.0 instead of 3.0, and this position minimizes the engine face circumferential DC_{60} distortion as indicated in Fig. 11. In comparing Figs. 21 and 23, it is apparent that the installation effect of locating the vortex generator configuration at the 'optimum' axial position is to 'spread out' the low energy flow at the engine face in a still more uniform pattern, thus lowering the DC_{60} distortion further. Again, this had consequences on the limiting streamlines, as can be seen by comparing Figs. 22 and 24. What is most remarkable is that small distortion differences show up very distinctly in the limiting streamline patterns induced by three vortex generator configurations. Thus surface flow patterns can prove invaluable in elucidating certain essential features of installed vortex generator performance, and they are very easy to obtain within experimental studies.

Thus, vortex flow control of inlet distortion can also be viewed as creating a new secondary flow field structure that will redistribute the low energy flow at the engine face in a more uniform manner. Although mixing takes place between the high energy core flow and low energy boundary layer flow, the primary gains result as a consequence of this redistribution process.

CONCLUDING REMARKS

The present study demonstrates that the Reduced Navier Stokes code RNS3D can be used very effectively to develop a vortex generator installation for the purpose of minimizing the engine face circumferential distortion by controlling the development of secondary flow. The computing times required are small enough that studies such as this are feasible within a design environment with all its constraints of time and costs.

In this preliminary research study, computational fluid dynamics (CFD) was used to investigate the management of inlet distortion by the introduction of discrete vorticity sources at selected locations in the inlet for the purpose of controlling secondary flow. These sources of vorticity were introduced by means of vortex generators. A series of design observations were made concerning the importance of various vortex generator design parameters in minimizing engine face circumferential distortion. The study showed that vortex strength, generator scale, and secondary flow field structure have a complicated and interrelated influence on the engine face distortion, over and above the initial geometry and arrangement of the generators. Overall, the installed vortex generator performance was found to be a function of three categories of variables, namely: (1) the inflow conditions, i.e. throat Mach number (inlet mass flow), Reynolds number, etc., (2) the aerodynamic characteristics associated with the inlet duct, and (3) the design parameters related to the geometry, arrangement, and placement of the vortex generators within the inlet duct itself. The design challenge on the one hand, is to view vortex flow control as an an integral part of the inlet design, and on the other hand to manage simultaneously all of the design variables in an integrated fashion in order to enlarge the flight envelope of the aircraft under consideration.

REFERENCES

1. Advisory Group for Aerospace Research and Development (AGARD), "Engine Response to Distorted Inflow Conditions," AGARD CP-400, Sept., 1986.

2. Bowditch, D. N. and Coltrin, R. E., "A Survey of Inlet/Engine Distortion Compatability," AIAA Paper No. 83-1166, June 1983.

3. Taylor, D., "Application of Vortex Generator Mixing Principle to Diffusers," U.A.C. Rep. R-15064-5, Dec. 1948.

4. Valentine, E. F. and Carrol, R. B., "Effects of Several Arrangements of Rectangular Vortex Generators on the Static Pressure Rise Through a Short 2:1 Diffuser," NASA RM L50L04, Feb. 1951.

5. Valentine, E. F. and Carrol, R. B., "Effects of Some Primary Variables of Rectangular Vortex Generators on the Static Pressure Rise Through a Short Diffuser," NACA RM 52B13, May 1952.

6. Pearcy, H. H. and Stuart, C. M., "Methods of Boundary-Layer Control for Postponing and Alleviating Buffeting and other Effects of Shock-Induced Separation," Presented at the IAS National Summer Meeting, Los Angeles, Calf., June 1959.

7. Kaldschmidt, G., Syltedo, B. E., and Ting, C. T., "727 Airplane Center Duct Inlet Low-Speed Performance Confirmation Model Test for Refanned JT8D Engines - Phase II," NASA CR-134534, Nov. 1973.

8. Anderson, B. H., "The Aerodynamic Characteristics of Vortex Ingestion for the F/A-18 Inlet Duct," AIAA Paper No. 91-0130, Jan. 1991.

9. Anderson, B. H. and Levy, R., "A Design Strategy for the Use of Vortex Generators to Manage Inlet-Engine Distortion Using Computatinal Fluid Dynamics," AIAA Paper No. 91-2474, June 1991.

10. Anderson, B. H. and Farokhi, S.,"A Study of Three Dimensional Turbulent Boundary Layer Separation and Vortex Flow Control Using the Reduced Navier Stokes Equations," Turbulent Shear Flow Symposium, Munich, Germany, Sept. 1991.

11. Anderson, B. H. and Levy, R.,"Vortex Generator Design for Aircraft Inlet Distortion as a Numerical Optimization Problem," Conference on Inverse Design Concepts and Optimization in Engineering Sciences-III (ICIDES-III), Oct. 1991.

12. Briley, W. R. and McDonald, H., "Analysis and Computation of Viscous Subsonic Primary and Secondary Flow," AIAA Paper No. 79-1453.

13. Briley, W. R., and McDonald, H., "Three-Dimensional Viscous Flows with Large Secondary Velocities," Journal of Fluid Mechanics, March 1984, vol. 144, pp. 47-77.

14. Kreskovsky, J. P., Briley, W. R. and McDonald, H., "Prediction of Laminar and Turbulent Primary and Secondary Flows in Strongly Curved Ducts," NASA CR-3388, Feb. 1981

15. Levy, R., Briley, W. R., and McDonald, H., "Viscous Primary/Secondary Flow Analysis for Use with Nonorthogonal Coordinate Systems," AIAA Paper No. 83-0556, Jan. 1983.

16. Towne, C. E., and Anderson, B. H., "Numerical Simulation of Flows in Curved Diffusers with Cross-Sectional Transitioning Using a Three Dimensional Viscous Analysis," AIAA Paper No. 81-0003, Jan. 1981.

17. Towne, C. E., "Computation of Viscous Flow in Curved Ducts and Comparision with Experimental Data," AIAA Paper No. 84-0531, Jan. 1984.

18. Anderson, B. H., "Three Dimensional Viscous Design Methodology of Supersonic Inlet Systems for Advanced Technology Aircraft," Numerical Methods for Engine-Airframe Integration, American Institute of Aeronautics and Astronautics Series, 1986.

19. Kunik, W. G., "Application of a Computational Model for Vortex Generators in Subsonic Internal Flows," AIAA Paper No. 86-1458, June 1986.

20. Squire, R., "Growth of a Vortex in Turbulent Flow," The Aeronautical Quarterly, Vol. 16, Pt. 3, August 1965, pp 302-306.

21. McDonald, H. and Camarata, F. J., "An Extended Mixing Length Approach for Computing the Turbulent Boundary-Layer Development, Proceedings, Stanford Conference on Turbulent Boundary Layers," Vol. I, Stanford University, pp. 83-98, 1969.

22. Horlock, J. H. and Lakshminarayana, B., "Secondary Flows: Theory, Experiment, and Applications in Turbomachinery Aerodynamics," Ann. Rev. Fluid Mechanics, Vol 5, pp 247-280.

23. Lakshminarayana, B., and Horlock, J. H., "Generalized Expressons for Secondary Vorticity Using Intrinsic Coordinates," J. Fluid Mechanics. Vol. 59, pp 97-115.

24. Huang, P. S, and Piccolo, A., "Boeing 727 Re-Engining Center Inlet S-Duct," Dee Howard Rept. 102,-70, June, 1990.

25. Huang, P. S, Piccolo, A., Pascal, W. and Anderson., B. H., "Design and Analysis of Reengine Boeing 727-100 Center Inlet S-Duct by a Reduced Navier Stokes Code," AIAA Paper No. 92-1221, 1992.

26. Willmer, A. C., Brown, T. W., and Goldsmith, E. L., "Effects of Intake Geometry on Circular Pitot Intake Performance at Zero and Low Forward Speeds," Aerodynamics of Power Plant Installation, AGARD CP301, Paper No. 5, 1981.

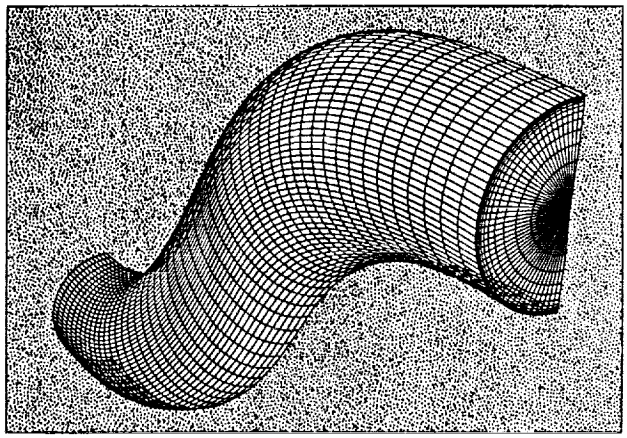

Fig. (1) Geometry definition for the 727/TAY651 54 center inlet duct.

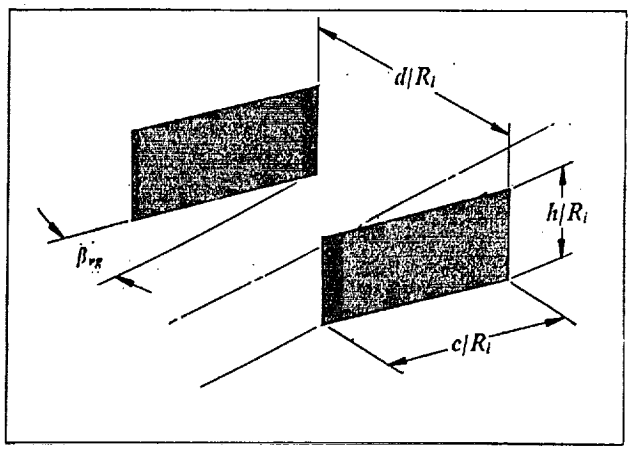

Fig. (2) Geometry definition of co-rotating vortex generators.

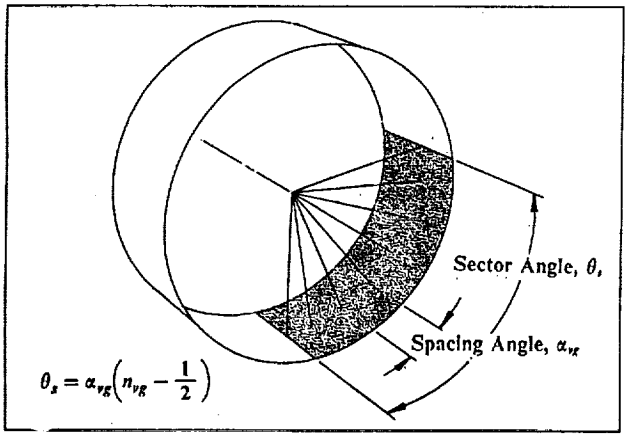

Fig. (3) Nomenclature used for vortex generator positioning.

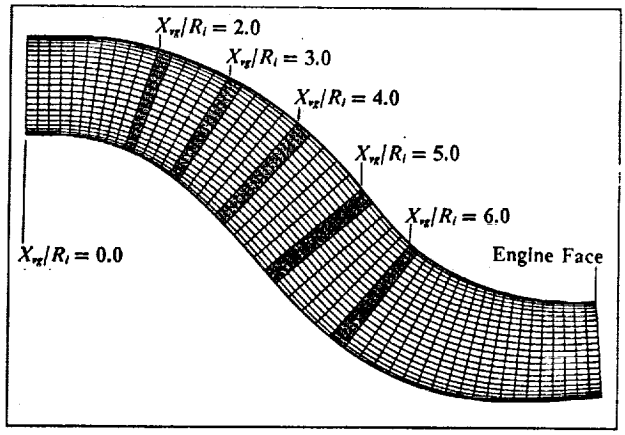

Fig. (4) Axial locations of the vortex generator sector regions.

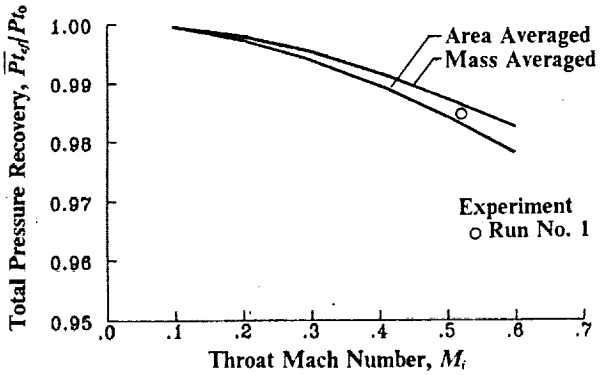

Fig. (5) Comparision between measured and calculated engine face total pressure recovery for the 727/TAY651 54 center inlet duct without vortex flow control.

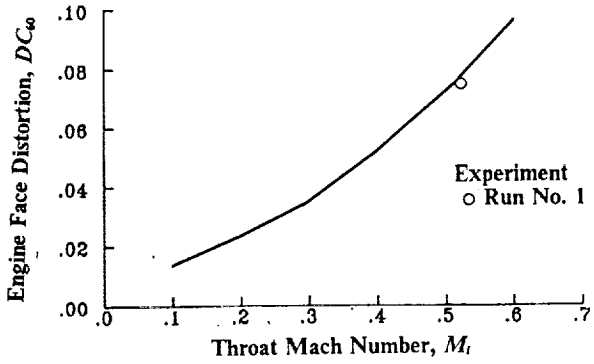

Fig. (6) Comparision between measured and calculated engine face DC_{60} distortion for the 727/TAY651-54 center inlet duct without vortex flow control.

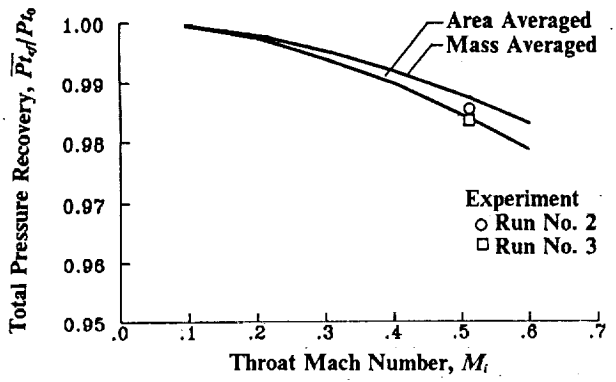

Fig. (7) Comparision between measured and calculated engine face pressure recovery for the 727/TAY651-54 center inlet duct, with vortex flow control.

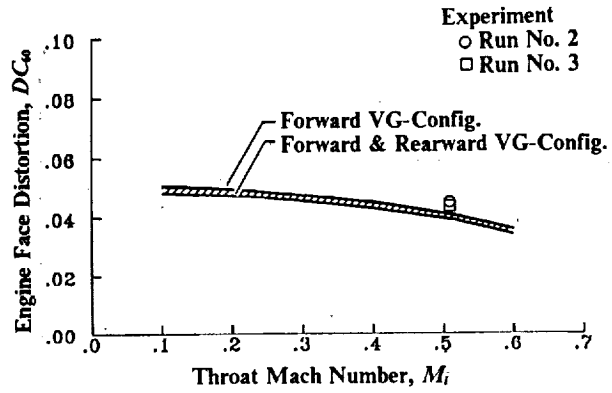

Fig. (8) Comparision between measured and calculated engine face DC_{60} distortion for the 727/TAY651-54 center inlet duct, with vortex flow control.

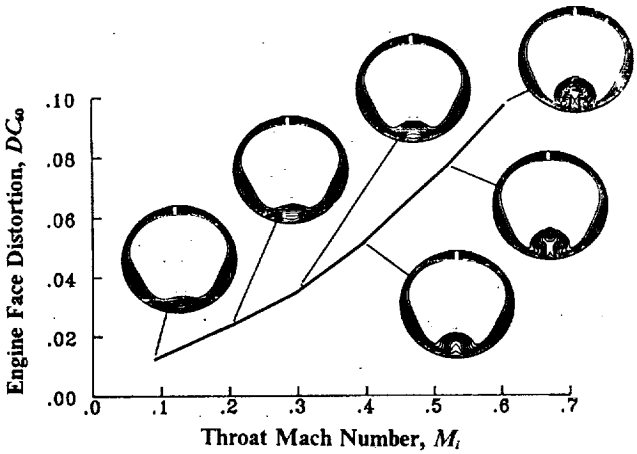

Fig. (9) Effect of inlet throat Mach number (M_i) on engine face DC_{60} distortion for the 727/TAY651-54 center inlet duct without vortex flow control.

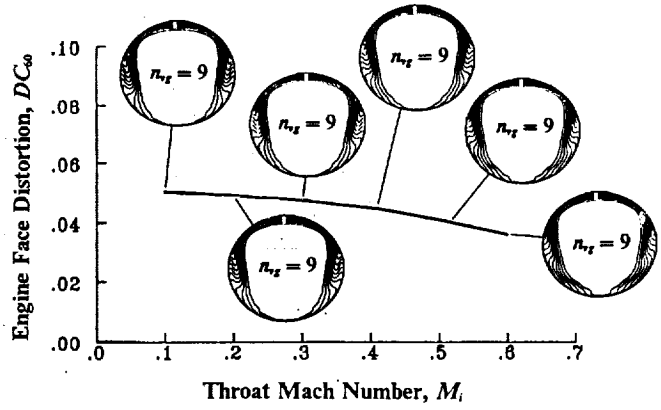

Fig. (10) Effect of inlet throat Mach number (M_i) on engine face DC_{60} distortion for the 727/TAY651-54 center inlet duct, with vortex flow control.

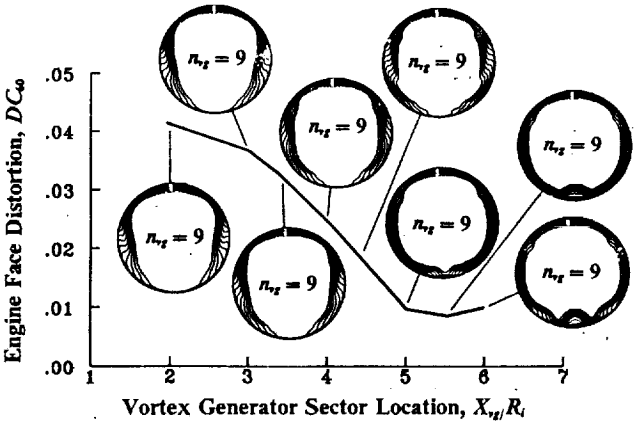

Fig. (11) Effect of vortex generator installation axial sector location (X_{vg}/R_i) on engine face DC_{60} distortion.

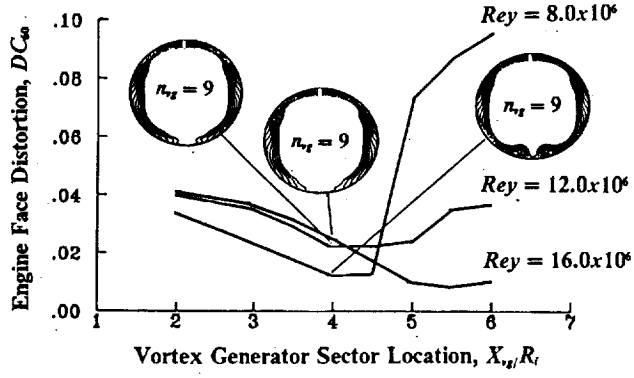

Fig. (12) Effect of Reynolds number on the optimum vortex generator axial installation location.

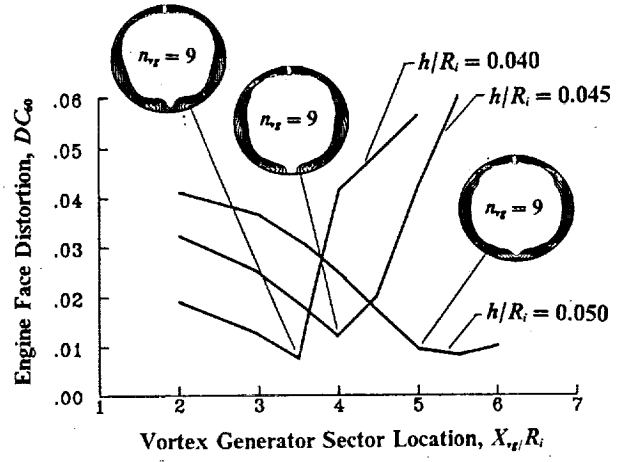

Fig. (13) Effect of generator blade height (h/R_i) on the optimum vortex generator axial installation location.

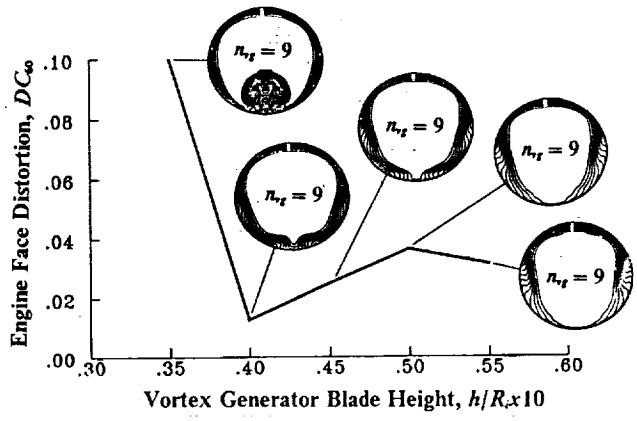

Fig. (14) Effect of generator blade height (h/R_i) on engine face DC_{60} distortion for the generator installation located at $X_{vg}/R_i = 3.0$.

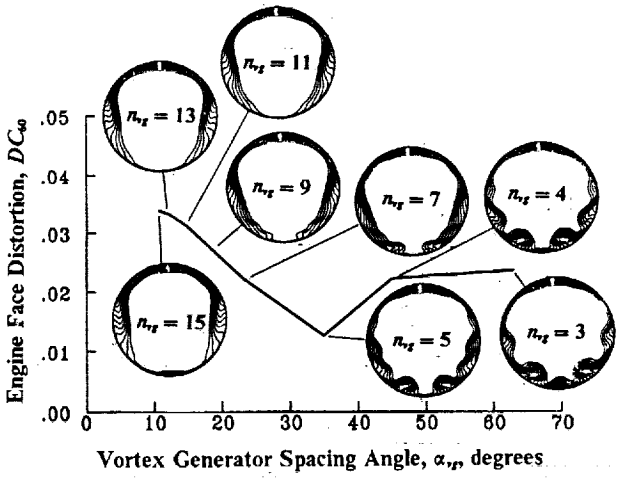

Fig. (15) Effect of generator spacing angle (α_{vg}) on engine face DC_{60} distortion for the generator installation located at $X_{vg}/R_i = 3.0$.

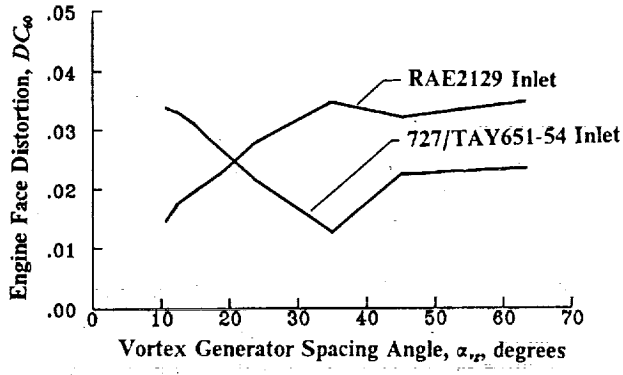

Fig. (16) Effect of inlet geometry on optimum spacing angle (α_{vg}) for the generator installation located at $X_{vg}/R_i = 3.0$.

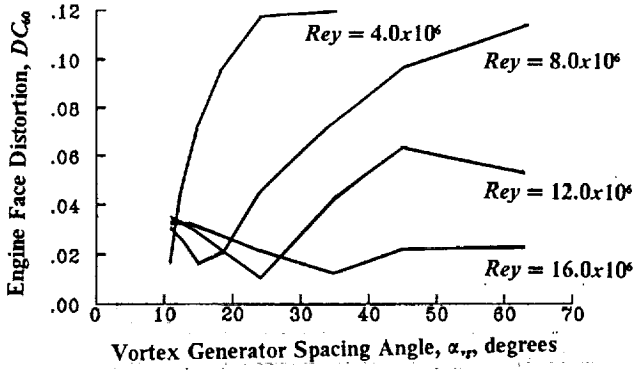

Fig. (17) Effect of inlet Reynolds number on the optimum spacing angle (α_{vg}) for the generator installation located at $X_{vg}/R_i = 3.0$.

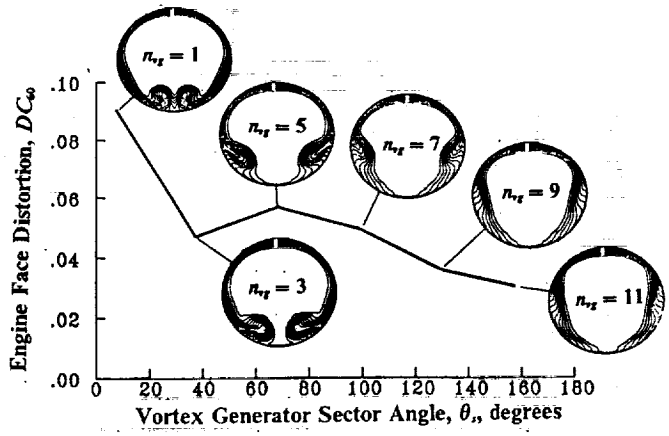

Fig. (18) Effect of generator sector angle (θ_{vg}) on engine face DC_{60} distortion for the generator installation located at $X_{vg}/R_i = 3.0$.

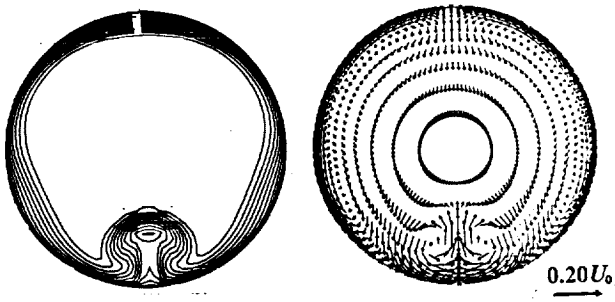

Fig. (19) Engine face flow field for the 727/TAY651-54 center inlet duct without vortex generators.

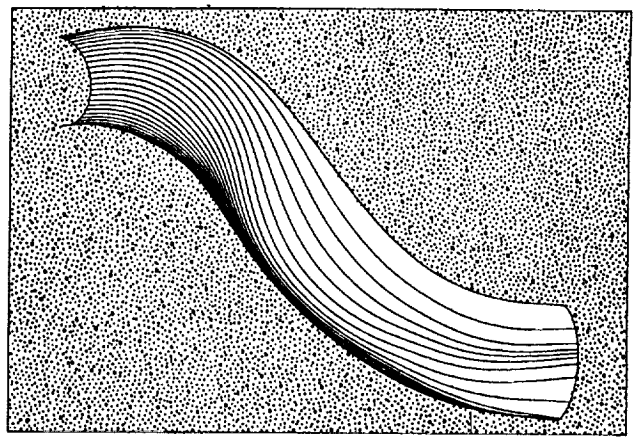

Fig. (20) Reduced Navier Stokes (RNS) solution showing the limiting streamline patterns for the 727/TAY651-54 center inlet duct without vortex generators.

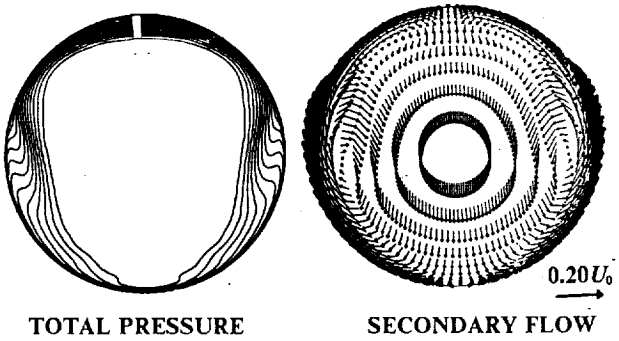

Fig. (21) Engine face flow field for the 727/TAY651 54 center inlet duct, generator configuration dh729.

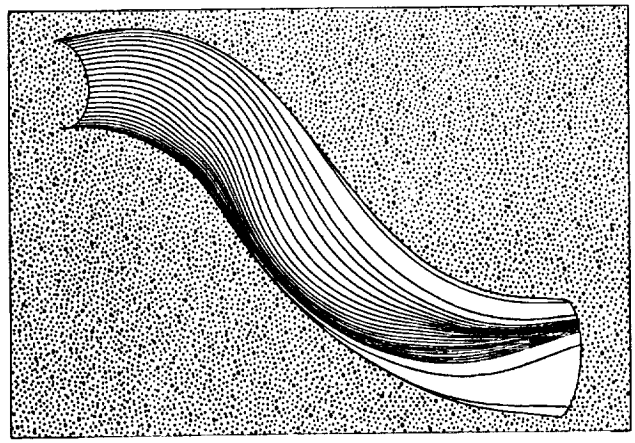

Fig. (22) Reduced Navier Stokes (RNS) solution showing the limiting streamline patterns for the 727/TAY651-54 center inlet duct, generator configuration dh729.

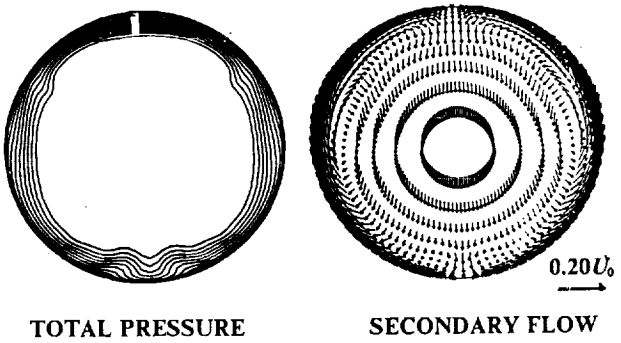

Fig. (23) Engine face flow field for the 727/TAY651-54 center inlet duct, generator configuration dh733.

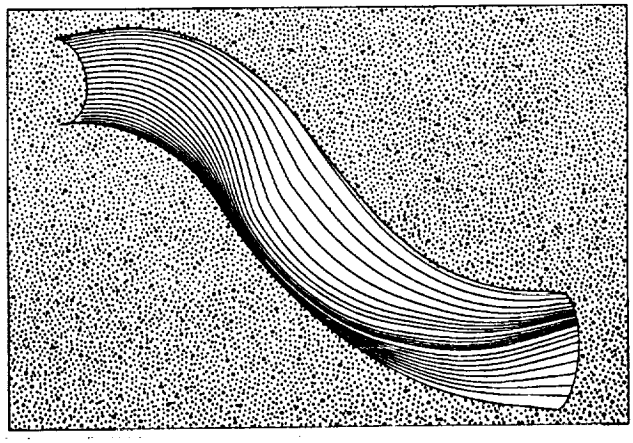

Fig. (24) Reduced Navier Stokes (RNS) solution showing the limiting streamline patterns for the 727/TAY651-54 center inlet duct, generator configuration dh733.

REPORT DOCUMENTATION PAGE

Form Approved
OMB No. 0704-0188

1. AGENCY USE ONLY (*Leave blank*)	2. REPORT DATE	3. REPORT TYPE AND DATES COVERED
	1991	Technical Memorandum

4. TITLE AND SUBTITLE

A Study on Vortex Flow Control on Inlet Distortion in the Re-Engined 727-100 Center Inlet Duct Using Computational Fluid Dynamics

5. FUNDING NUMBERS

WU - 505 - 62 - 52

6. AUTHOR(S)

Bernhard H. Anderson, Pao S. Huang, William A. Paschal, and Enrico Cavatorta

7. PERFORMING ORGANIZATION NAME(S) AND ADDRESS(ES)

National Aeronautics and Space Administration
Lewis Research Center
Cleveland, Ohio 44135 - 3191

8. PERFORMING ORGANIZATION REPORT NUMBER

E - 6679

9. SPONSORING/MONITORING AGENCY NAMES(S) AND ADDRESS(ES)

National Aeronautics and Space Administration
Washington, D.C. 20546 - 0001

10. SPONSORING/MONITORING AGENCY REPORT NUMBER

NASA TM - 105321
AIAA - 92 - 0152

11. SUPPLEMENTARY NOTES

Prepared for the 30th Aerospace Sciences Meeting and Exhibit sponsored by the American Institute of Aeronautics and Astronautics, Reno, Nevada, January 6 - 9, 1992. Bernhard H. Anderson, NASA Lewis Research Center; Pao S. Huang, William A. Paschal, and Enrico Cavatorta, The Dee Howard Company, San Antonio, Texas 78217. Responsible person, Bernhard H. Anderson, (216) 433 - 5822.

12a. DISTRIBUTION/AVAILABILITY STATEMENT

Unclassified - Unlimited
Subject Categories 02 and 07

12b. DISTRIBUTION CODE

13. ABSTRACT (*Maximum 200 words*)

In this preliminary research study, computational fluid dynamics (CFD) was used to investigate the management of inlet distortion by the introduction of discrete vorticity sources at selected locations in the inlet for the purpose of controlling secondary flow. The sources of vorticity were introduced by means of vortex generators. A series of design observations were made concerning the importance of various vortex generator design parameters in minimizing engine face circumferential distortion. The study showed that vortex strength, generator scale, and secondary flow field structure have a complicated and interrelated influence on the engine face distortion, over and above the initial geometry and arrangement of the generators. Overall, the installed vortex generator performance was found to be a function of three categories of variables, namely: (1) the inflow conditions, i.e. throat Mach number (inlet mass flow), Reynolds number, etc., (2) the aerodynamic characteristics associated with the inlet duct, and (3) the design parameters related to the geometry, arrangement, and placement of the vortex generators within the inlet duct itself.

14. SUBJECT TERMS

Applied aerodynamics; Computational fluid dynamics; Internal flow

15. NUMBER OF PAGES

14

16. PRICE CODE

A03

17. SECURITY CLASSIFICATION OF REPORT	18. SECURITY CLASSIFICATION OF THIS PAGE	19. SECURITY CLASSIFICATION OF ABSTRACT	20. LIMITATION OF ABSTRACT
Unclassified	Unclassified	Unclassified	